ESCUELA TÉCNICA SUPERIOR DE INGENIERÍA INFORMÁTICA

INGENIERÍA DE LA SALUD: MENCIÓN EN INGENIERÍA BIOMÉDICA

ESTUDIO DE LA CORRELACIÓN ENTRE LA PRESENCIA DE VÁLVULA AÓRTICA BICÚSPIDE Y EL DESARROLLO DE DISECCIÓN AÓRTICA.

STUDY OF THE CORRELATION BETWEEN BICUSPID AORTIC VALVE AND THE DEVELOPMENT OF AORTIC DISSECTION.

Realizado por
ELVIRA RUIZ JIMÉNEZ
Tutorizado por
LUIS PARRAS ANGUITA
SARAH C. VIGMOSTAD
Departamento
MECÁNICA DE FLUIDOS

UNIVERSIDAD DE MÁLAGA

MÁLAGA, enero 2015

Fecha defensa:
El Secretario del Tribunal

RESUMEN

Resumen: La disección aórtica (AD) es la condición letal más comúnmente diagnosticada de la arteria aorta y consiste en el redireccionamiento del flujo sanguíneo desde el lumen de la aorta hasta la media de la pared de la aorta a través de una pequeña fisura en la intima. Las causas específicas de la formación de esta fisura, y de la subsecuente dilatación de la pared, todavía no han sido completamente determinadas aunque diversos estudios muestran que puede ser debida o bien a cambios químicos o bien a efectos mecánicos en la pared de la aorta. Este trabajo se centra en el estudio de posibles efectos mecánicos, inducidos por cambios en la hemodinámica de la arteria, que puedan haber conducido al debilitamiento de la pared de la aorta. Válvula aórtica bicúspide (BAV) es la enfermedad congénita del corazón más común y se ha demostrado su importante contribución en el desarrollo de numerosas condiciones cardiovasculares. Esta enfermedad modifica el orificio de salida del corazón, y por tanto el perfil hemodinámico de eyección, del flujo de sangre, lo que podría tener consecuencias en el comportamiento mecánico de la pared de la aorta. Este estudio tiene como objetivo determinar que existe una correlación entre los cambios en la hemodinámica producidos por la presencia de BAV y la formación de AD usando técnicas de análisis de dinámica de fluidos computacional (CFD). Para determinar dicha relación, análisis CFD se han realizado en tres geometrías diferentes: un caso de válvula aórtica tricúspide (TAV) y dos casos distintos de BAV. Todas las geometrías son idealizadas y contemplan la raíz de la aorta, la aorta ascendente y el comienzo del cayado aórtico. Los resultados de los análisis muestran un incremento en la velocidad de eyección de la sangre para ambos casos de BAV debido a la reducción en el área efectiva del orificio. Además, el estudio muestra un incremento en las fuerzas de rozamiento de la pared y en la presión de la pared externa de la aorta. Estos resultados nos llevan a la conclusión de que BAV podría causar hipertensión en la pared externa de la aorta, la cual es una causa mecánica conocida del debilitamiento de vasos sanguíneos.

Palabras claves: ingeniería biomédica, disección aórtica, válvula aórtica bicúspide, patología cardiovascular, análisis CFD, dinámica de fluidos computacional, hemodinámica, biomecánica cardiovascular.

ABSTRACT

Abstract: Aortic Dissection (AD) is the most commonly diagnosed lethal condition of the aorta and it consists on the redirection of the blood from the lumen of the aorta to the media of the aortic wall through a tear on the intima. The specific cause of the formation of the tear, and subsequent dilatation of the wall, has not been fully determined yet, however, studies show that it can be due to either chemical changes or mechanical effects on the aortic wall. This thesis will focus on possible mechanical effects, induced by changes in the haemodynamics of the aorta, which could potentially lead to weakening of the aortic wall. Bicuspid Aortic Valve (BAV) is the most common congenital heart diseases and it has been proven to have a significant role on the development of several cardiovascular conditions. This condition modifies the outlet orifice, modifying therefore the ejection profile of the blood flow, which could have consequences on the mechanical behavior of the aortic wall. This study aims to determine that there is a correlation between the changes in haemodynamics produced by BAV and the formation of AD using computational fluid dynamics techniques. In order to assess this correlation, CFD analyses have been performed in three different geometries: a Tricuspid Aortic Valve (TAV) case and two different cases of BAV. All three geometries are idealized and take into consideration the aortic root, the ascending aorta and the beginning of the aortic arch. The results from the analyses show an increment in the ejection velocity of the blood for both BAV cases due to the reduction on the effective orifice area. In addition, an increment in wall shear stress and pressure on the outer wall in respect to the TAV case has also been found. These results lead to the conclusion that BAV could cause hypertension in the outer wall of the aorta, which is known to be a mechanical cause of weakening of the blood vessels.

Keywords: biomedical engineering, aortic dissection, bicuspid aortic valve, cardiovascular pathology, CFD analysis, computational fluid dynamics, haemodynamics, cardiovascular biomechanics.

TABLE OF CONTENTS

LIST OF FIGURES

THESIS

INTRODUCTION

1.1 Background

1.1.1 Physiology of the human heart

The heart is the most important organ in the cardiovascular system. It pumps the blood through out the entire body, allowing the transport of nutrients and oxygen to the cells and muscles. It is divided in four main chambers called left ventricle, left atrium, right ventricle and right atrium (see figure 1a).

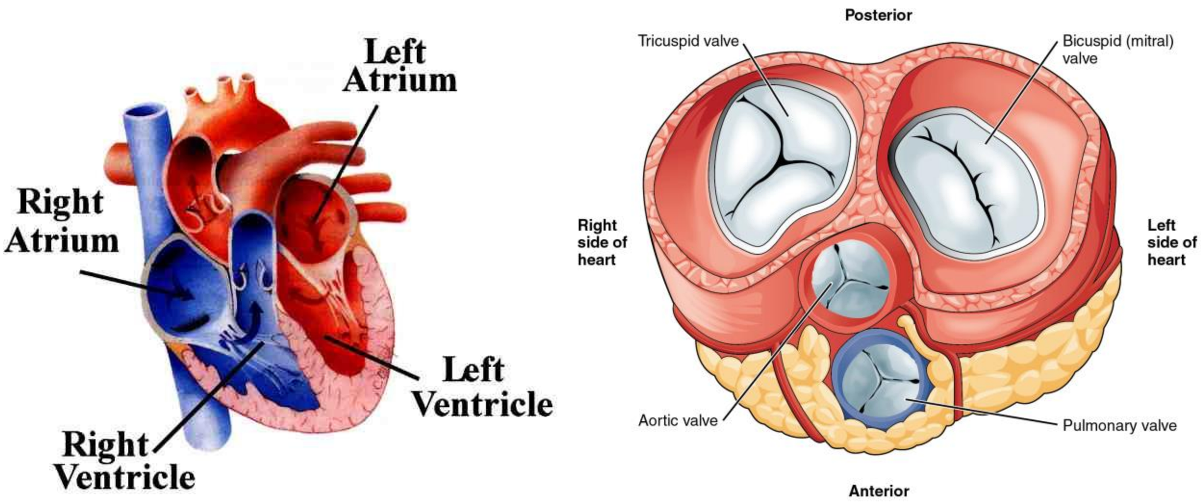

Figure 1. Representation of the (a) heart chambers[6] and (b) heart valves[5].

The blood flow throughout the heart is controlled with four valves (see figure 1b) which are formed by pieces of tissue called leaflets and which main function is to keep the flow unidirectional. The valves can be classified as:

- **Mitral valve:** formed by two leaflets, divides the left atrium from the left ventricle and it prevents blood to regurgitate into the atrium during the stroke.
- **Tricuspid valve,** formed by three leaflets, divides right atrium and right ventricle and prevents blood regurgitate to the atrium during the stroke.
- **Pulmonary valve,** formed by three leaflets, situated at the beginning of the pulmonary artery, prevents blood to flow back to the right ventricle.
- **Aortic valve,** formed by three leaflets, situated at the entrance of the ascending aorta, prevents blood to flow back to the left ventricle.

Each valve is able to resist different levels of pressure, allowing for some to be open while others remain closed in different parts of the cardiac cycle.

1.1.2 Physiology of the aorta

The aorta is the largest artery of the body and it conducts the blood from the heart into the systemic circulation. It can be divided into four different sections (see figure 2a):

- **Aortic root:** region that connects the heart with the ascending aorta.
- **Ascending aorta:** region contained from the aortic root and until the beginning of the aortic arch.
- **Aortic arch:** section of the aorta with the shape of an inversed U, it covers from the end of the ascending aorta and until the beginning of the descending aorta.
- **Descending aorta:** region of the aorta that initiates at the end of the aortic arch and evolves into the division of the aorta in femoral arteries. The descending aorta can itself be divided into thoracic aorta, part of the aorta that is under the diaphragm, and abdominal aorta, region contained from the thoracic aorta and until the bifurcation.

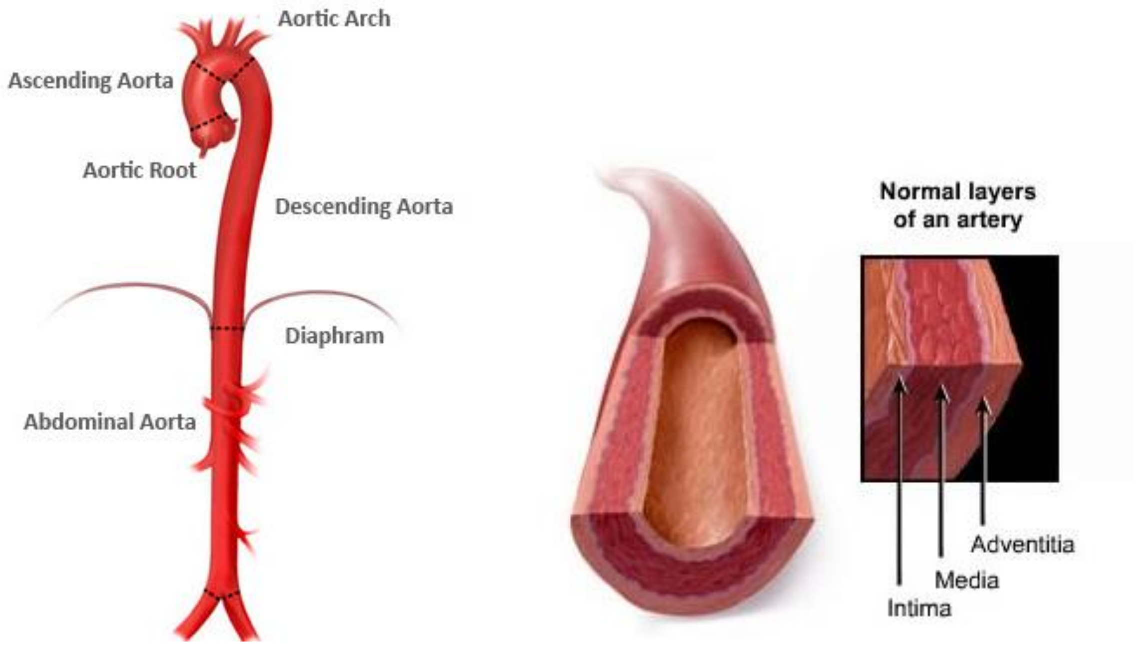

Figure 2. Representation of the (a) regions of the aorta[7] and (b) the layers of the wall[8].

The aorta is composed mainly by muscle cells, elastin and collagen, which are organized into three layers[1] (see figure 2b):

- **Intima:** is the internal elastic lamina. Formed by endothelial cells.
- **Adventitia:** external elastic lamina formed by mainly collagen.
- **Media:** smooth muscle cells.

1.1.3 Physiology of the aortic root

The aortic root connects the heart to the systemic circulation and it is composed by the aortic valve leaflets, the leaflets attachments, the sinuses of Valsalva, the interleaflet trigones, the sinotubular junction and the annulus (see figure 3)[10].

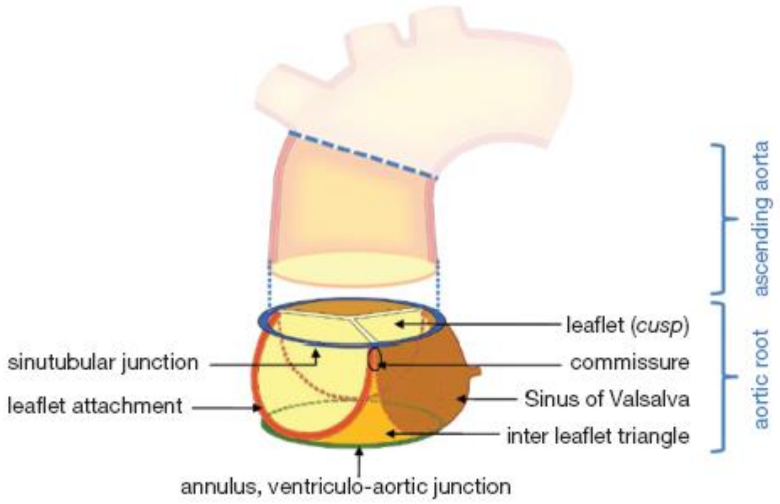

Figure 3. Scheme of the aortic root.[10]

.

- **Aortic valve leaflets:** as previously explained, this is a pressure-drive closing/opening mechanism formed by three thin pieces of tissue called leaflets and it constitutes the hemodynamic (as well as physical) point of transition from the heart to the systemic circulation. This means that from this point into the artery, the structures would be subjected to arterial pressure and hemodynamics; while from this point into the heart, the structures are subjected to ventricular pressure and hemodynamics. There are studies that indicate that the geometric design of the leaflets leads to “the optimal solution for low resistance valve configuration”[10].
- **Leaflets attachments:** the leaflets insert in the wall of the aortic root forming a crown shaped structure. The region where they run parallel is called commissures.
- **Sinuses of Valsalva:** formed by the three symmetric bulges of the aortic wall. Their precise function is yet unclear although they connect the aorta with the coronary arteries. Each one of the sinuses has been named accordingly with the arteries they connect to: left, right and non coronary sinus.
- **The interleaflet triangles:** situated under each commissures, they are consider haemodynamically as “extensions of the ventricular outflow tract”[10].

- **Sinotubular junction:** formed by the distal part of the sinuses and the commissures, separates the aortic root from the ascending aorta.
- **Annulus:** area where the blood path between the left ventricle and the aorta has the smallest diameter[10].

1.1.4 Pathophysiology of Aortic Dissection

Thoracic aortic dissection is a serious condition produced when blood enters the media of the aortic wall through a tear in the intima. This produces an abnormal growth on the media, separating the intima and adventitia along a variable length.[2]

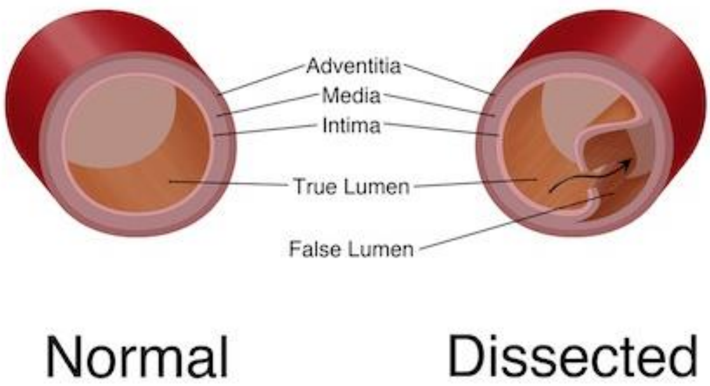

Figure 4. Comparison between a normal and a dissected aorta.[9]

Aortic dissection can be anatomically classified based on its location and extension following one of the two following criteria: Stanford classification and DeBakey classification[2,4].

- **Stanford classification:** it divides dissections into type A (those that involve the ascending aorta) and type B (those that doesn't involve the ascending aorta). This classification system will be used through out this study.
- **DeBakey classification:** divides dissections into type I (involve the ascending aorta, aortic arch and descending aorta); type II (restricted to the ascending aorta); and type III (restricted to the descending aorta).

Aortic dissection can be considered acute, if the dissection has occurred within the first 2 weeks after the development of the intimal tear; or chronic, if the dissection appears more that 2 months after the formation of the tear. Often patients don't survive the acute form (almost 40% die immediately[2]), and those who survive passed on to developing chronic dissection.

Thoracic aortic dissection is currently diagnosed using computerized tomography and echocardiography.

1.1.5 Pathophysiology of Bicuspid Aortic Valve

The possible causes of aortic dissection go from abnormality in the biomechanics within the media to direct mechanical forces on the wall. However, one of the main non-traumatic possible causes of this is the stress variation in the aortic wall due to changes in the haemodynamics. These changes can be caused, among other reasons, by anatomic changes in the aortic root.

A healthy aortic valve is formed by three leaflets, which produces a characteristic triangular shape when fully opened (figure 5). This shape allows the highest achievable area in the inlet, which leads to relatively low velocity. However, when a patient presents bicuspid valve, the aortic valve is said to present stenosis, the shape of the inlet becomes more oval, which produces a lower area, consequently increasing the velocity and lowering the pressure.

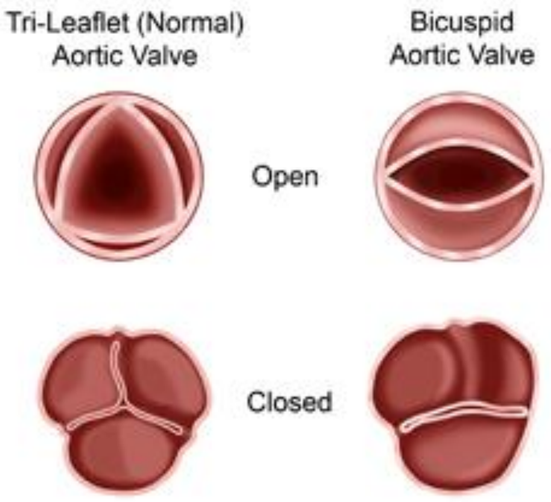

Figure 5. Representation of a tricuspid valve and a bicuspid valve both fully open and closed.[11]

Apart from changing the area, the presence of bicuspid valves would also affect the ejection profile, altering the area of impact in the wall of aorta. This could have a mechanical effect (in a macro or/and micro level) that would lead to the formation of aortic dissection.

There are several types of BAV (figure 6) depending on the number of raphes (the fused area of the junction of two leaflets) and the spatial location of the leaflets that are joined. This classification is based on a study by Sievers H. & Schmidtke C. published in Surgery for Acquired Cardiovascular Disease on 2007, which took into account 304 surgical specimens.[17]

- **Type 0:** this type presents no raphes and two fully developed leaflets of approximately the same area. It is also called the purely BAV. It can be subdivided into vertical or horizontal. Only ~7% of the BAV cases are type 0.
- **Type 1:** it is characterized for one raphe, which can be between the left and right coronary leaflets, the right and non-coronary leaflets, or the left and non-coronary leaflets. Approximately 88% of the studied BAV cases present this type of BAV.
- **Type 2:** characterized by two raphes formed between the left and right coronary leaflets and the right and non-coronary leaflets. Only about 5% of the studied cases present this kind of BAV.

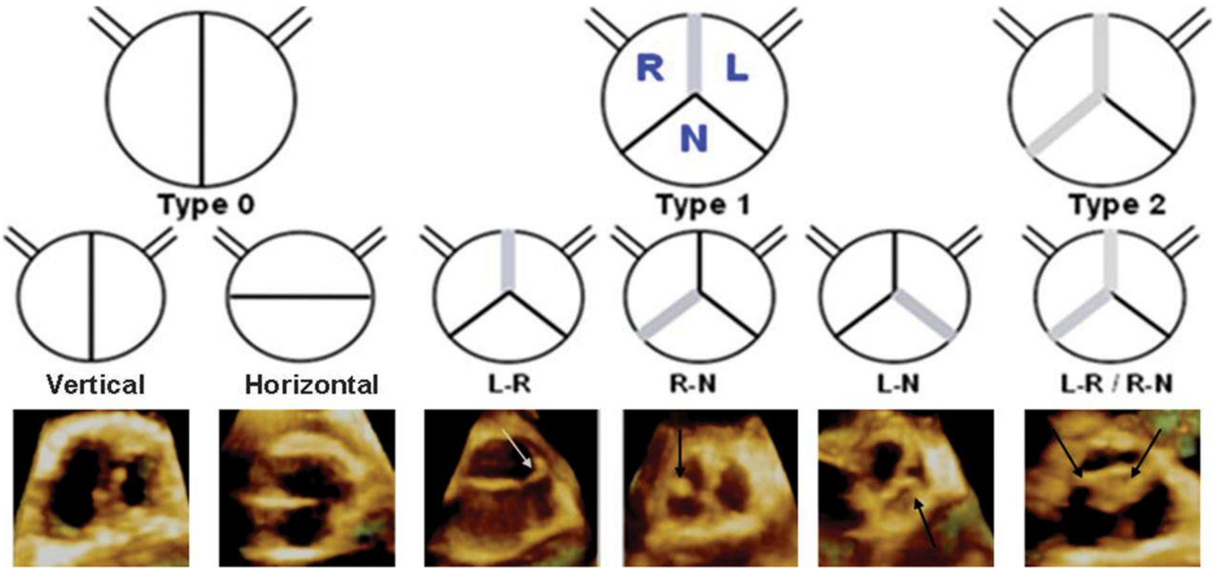

Figure 6. Correlation between schematics of the different types of BAV and 3D-TTE images.[13]

1.2 Motivation

Previous studies indicate that aortic dissection is "the most frequently diagnosed lethal condition of the aorta"[2] with statistics that estimate that this disease has an incidence between 2.9 and 3.5 per 100,000 per year in the USA[3].

On the other hand, Bicuspid aortic valve (BAV) is the most common congenital heart disease and it is widely related to several other cardiovascular complications.[12]

The association between bicuspid aortic valve and the dissection of the aorta has been identified as "BAD MATE" by Cotrufo et al[15]. Hemodynamic factors have been proposed to be a significantly important factor on this association, however, this hypothesis has been mostly based on indirect observational data.[12]

The relationship between bicuspid aortic valve and aortopathies has become increasingly important in the medical field, especially for surgical purposes. Nowadays, aortic dissection and several other types of aortopathies are treated with the use of stent grafts. However, it is not uncommon that some of these pathologies are directly related to bicuspid aortic valve. The study of the exact relationship between BAV and other pathologies could lead to the development of proactive treatments rather than reactive treatments, refocusing the treatments on fixing the cause of these diseases rather than the consequences. This could potentially lead to a lower rate of relapses, less and shorter visits to the hospital after the procedure and consequently a better quality o life for the patient.

Multiple studies on this field have been done focusing mainly on MRI examinations[12]. This study will however be focused on the use of computational fluid dynamics analysis tools on idealized geometries instead of patient specific. This will provide a more generalized idea of the changes in haemodynamics on a more controlled environment.

Due to the high percentage of BAV type 1 cases, this study will be focus on this kind but it is important to keep in mind that different types of bicuspid valves will produce different types of ejection profile, causing therefore different changes in the aortic wall. In addition, type A dissections are the most clinically common type of aortic dissection, which is why this study will focus on the hemodynamic changes that BAV produces in the ascending aorta and beginning of aortic arch.

METHODS AND PROCEDURE

This is a computational study focused on determining the relationship between the change in haemodynamics produced by bicuspid aortic valves, and the development of aortic dissection type A (Standford Classification).

2.1 Geometries

In this study, Computational Fluid Dynamics analyses have been performed on idealized geometries of the aortic root and arch (see figure 7). These geometries were designed by the Biomedical Engineering Department of The University of Iowa.

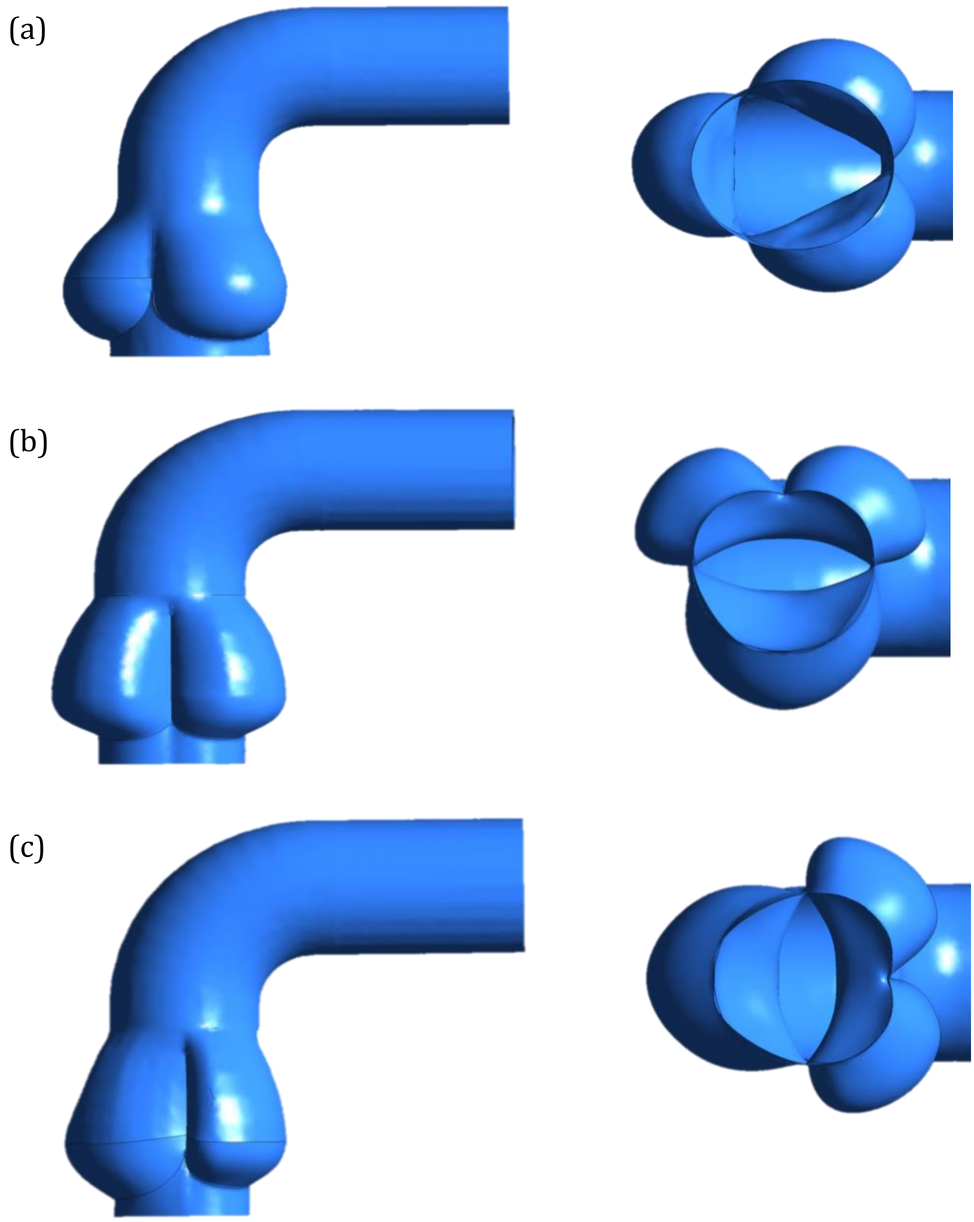

Figure 7. Lateral and bottom views of the geometry generated for a (a) tricuspid valve (b) BAV left-right fusion and (c) BAV left-non fusion.

Several bicuspid and tricuspid valves geometries from a previous finite element study were used as base, adding later on the remaining structures to complete the aortic root and arch. The geometric parameters of the models were assigned to match these geometries therefore they are off scale, with an outlet diameter of 1.23 cm. The flow properties will be adapted accordingly.

For this study, three different geometries have been utilized: two different cases of BAV type I (the most common), and one case of tricuspid valve. All three of these geometries represent the valves in peak systole, that is, fully opened. The aorta has been modeled as a cylindrical pipe to simplify the analysis and the cephalic arteries have not been considered.

Due to the change in the geometries of the leaflets, the sinuses also will vary accordingly, loosing their regular symmetric distribution, which could also affect the haemodynamics of the aorta.

Initially it was thought that the idealized geometries could be compared with patient specific geometries, however, after consulting Dr. Ben Jackson from The University of Pennsylvania he indicated that the techniques to obtain images to study the aorta and the aortic valve are very different. Therefore, it is really uncommon to have both images from the same patient, which leads to a pool of cases were each patient is really different from the other. Due to this limitation, it was decided that the study would only be made with idealized geometries.

2.2 Generation of the meshes

The three dimensional meshes for all the geometries were generated using Ansys Fluent 15.0 [Academic version] (see figure 8 (a) - (c)). The meshes are tetrahedral and the elements haven been set to have a minimum size of 1.e-5 m and a maximum size of 3.e-5 m. The size of the elements was decided taking into account the Reynolds number (Re) of the models. Boundary layer on a pipe has an approximate thickness of $D/\sqrt{Re}$, where D is the diameter of the model. The elements were scaled so the boundary layer would be formed by at least 1 element. Further refinement would be desirable but it is very computationally expensive. The number of elements implemented on each geometry is shown in table 1.

Geometry	**Number of elements**
Tricuspid Valve	504642
Bicuspid Valve – Type I – Left-Right fusion	359592
Bicuspid Valve – Type I – Left-Non fusion	359508

Table 1. Tetrahedral elements on each geometry.

Please notice that the considerably higher number of elements in the tricuspid valve mesh is due to several extra interfaces that were necessary to build the geometry but does not affect the results of the analysis.

(a) **(b)** **(c)**

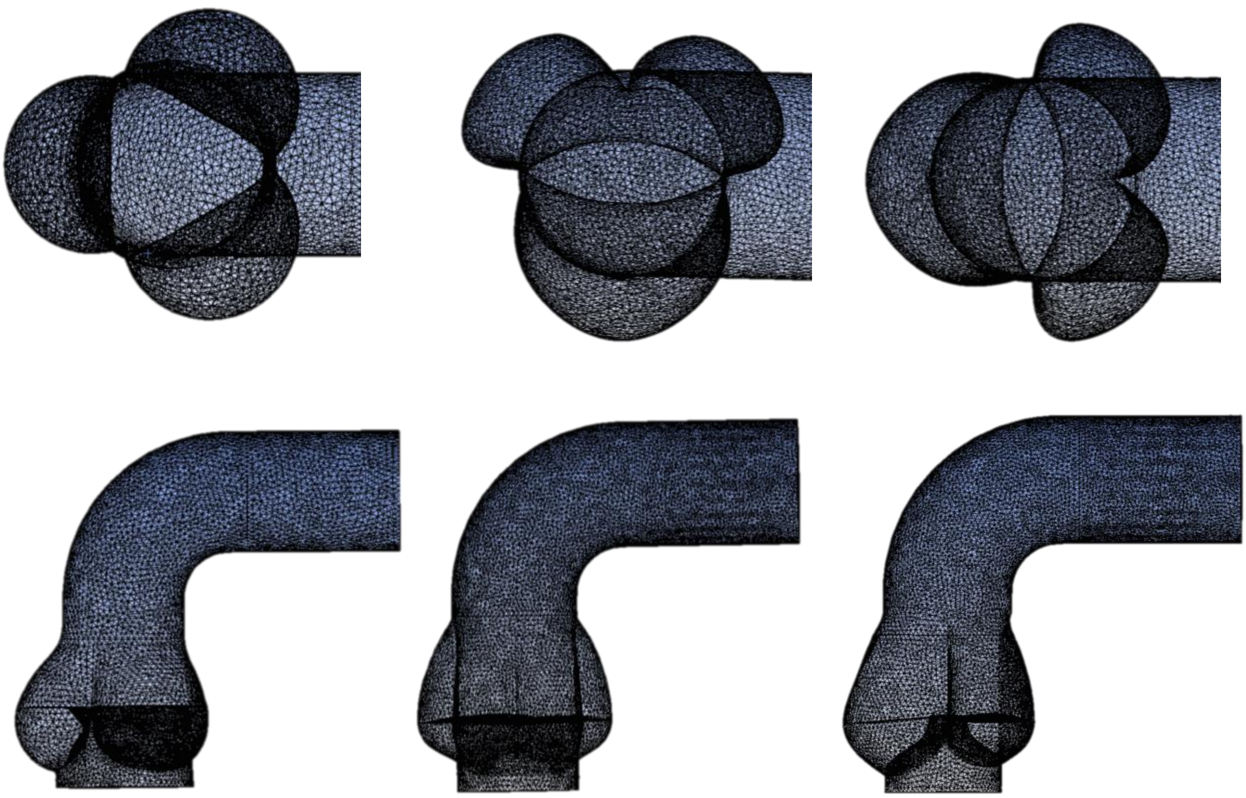

Figure 8. Bottom and lateral views of (a) the TAV mesh, (b) the BAV left-right mesh, and (c) the BAV left-non fusion mesh

2.3 Computational Fluid Dynamics Analysis

CFD analyses provide a faster and less invasive way of obtaining information about the blood flow. Apart form increasing the patience quality of life by diminishing the amount of time and money spent in the hospital, CFD presents less risks than in vivo studies. The use of this tool also potentially reduces the amount of animal experimentation and is more cost effective.

Once the meshes are correctly generated, they can be imported into Ansys Fluent 15.0, which uses Navier Stokes equations and the continuity equation to approximate a solution for the model based on parameters and inputs that have to be set. The Navier Stokes (momentum) and continuity equations for a three dimensional Newtonian incompressible flows are shown in equations 1 – 4.

*Momentum equation x-direction [**equation 1**]*

$$\rho g_x - \frac{\partial p}{\partial x} + \mu\left(\frac{\partial^2 u}{\partial x^2} + \frac{\partial^2 u}{\partial y^2} + \frac{\partial^2 u}{\partial z^2}\right) = \rho(\frac{\partial u}{\partial t} + u\frac{\partial u}{\partial x} + v\frac{\partial u}{\partial y} + w\frac{\partial u}{\partial z})$$

*Momentum equation y-direction [**equation 2**]*

$$\rho g_y - \frac{\partial p}{\partial y} + \mu\left(\frac{\partial^2 v}{\partial x^2} + \frac{\partial^2 v}{\partial y^2} + \frac{\partial^2 v}{\partial z^2}\right) = \rho(\frac{\partial v}{\partial t} + u\frac{\partial v}{\partial x} + v\frac{\partial v}{\partial y} + w\frac{\partial v}{\partial z})$$

*Momentum equation z-direction [**equation 3**]*

$$\rho g_z - \frac{\partial p}{\partial z} + \mu\left(\frac{\partial^2 w}{\partial x^2} + \frac{\partial^2 w}{\partial y^2} + \frac{\partial^2 w}{\partial z^2}\right) = \rho(\frac{\partial w}{\partial t} + u\frac{\partial w}{\partial x} + v\frac{\partial w}{\partial y} + w\frac{\partial w}{\partial z})$$

Continuity equation [**equation 4**]

$$\nabla \cdot \rho\vec{V} + \frac{\partial \rho}{\partial t} = 0$$

The assumptions utilized for the models of this study were the exact same on each case, leaving the change in geometries the only possible cause of differences in the obtained results. These assumptions are specified next.

2.3.1 Boundary conditions

This study distinguishes between the exterior surface of the aorta (which assigned boundary condition (B.C.) is going to be wall), the leaflets (wall), the inlet (velocity inlet with a velocity magnitude of 0.17 m/s) and the outlet of the aortic arch (pressure-outlet). The gauge pressure at the outlet has been set to 13332.2 Pa, the average systolic pressure, in order to obtain more accurate data. To simplify the model both the surface of the aorta and the leaflets have been assumed to be rigid walls.

2.3.2 Flow characteristics

Blood has been modeled as a Newtonian incompressible fluid, allowing the density to remain constant at 1102.9 kg/m^3. Even though the rheology of blood can be better described by Casson's relationship, the study of its viscous behavior determines that at relatively high rates of shear, viscosity approaches an asymptotic value.[1] Therefore, the assumption of constant viscosity in the aorta during systole, where high levels of shear stress are expected, seems to be acceptable. This viscosity constant has been set to 0.1 cP. The physiological values of the blood properties are 1060 kg/m^3 and 3.5 cP[1] for the density and the viscosity, respectively. These values have been adapted in our models so that the Reynolds number of the analyses matches that of the physiological case, due to the change in dimensions. This adaptation is only acceptable because we are treating the fluid as Newtonian, therefore the density and viscosity themself are not important, but the ratio of one over the other is.

The models have been modeled as unsteady laminar flows. Even though blood flow is pulsatile, this study only considers blood flow in systole; On the other hand, the geometry of the aortic root will produce some vortices in the sinuses that will make the flow unsteady, even if we set the inlet velocity to a constant 0.17 m/s. The peak ejecting velocity during systole has been estimated to be 0.7 m/s (based on a cardiac output of 20 L/min)[1], but this velocity is only present in the flow during a relatively short period of time. The study of the flow with this velocity would not yield realistic results of what happens in the aorta during systole. Instead, the analyses will be run with a mean time-averaged flow velocity of 0.17 m/s (based on a cardiac output of 5 L/min)[1]. Simplifying the flow as laminar (therefore neglecting any turbulence) can be justified by computing the Reynolds number using equation 5, where ρ is density (kg/m^3), u inlet velocity (m/s), D diameter of the aorta (m) and μ constant viscosity (kg/m $\cdot$s). Using the established numbers, an approximate Reynolds number of 1500 can be calculated (for both the physiological case and the models studied), which is well below the approximate limit of 2100 that determines that the inertial forces overcome the viscous forces and the flow becomes turbulent.

$$Re = \frac{\rho u D}{\mu} \qquad \textbf{[equation 5]}$$

It is important to notice that if the peak velocity were used, a Reynolds number of 5000 will be calculated. As explained before, this velocity is instantaneous, which means that the turbulent flow will not have time to develop before the velocity starts decreasing, so the flow remains laminar. This study has assumed transient flow but has set a constant inlet velocity, time-averaging the flow velocity, as a result of this, there is no need to match the Womersley number for the analyses.

The walls of the aorta have been considered rigid walls. Blood vessels are viscoelastic and distend with pulse pressure, what means that rigid wall would generally not be a valid assumption. However, to simplify this analysis, the radial velocity has been considered negligible and therefore the distention of the aorta has not been taken into account.

RESULTS

3.1 Streamlines

Pathlines generated for each one of the models is shown in figures 9 (a) – (c). These pathlines are colored by velocity magnitude. The results show great discrepancy between the models in terms of points of recirculation.

Changes in the haemodynamics of the aorta passed the sinuses are also visible. It is important to notice that the models for the two different types of bicuspid valves yield considerably different pathlines.

(a)

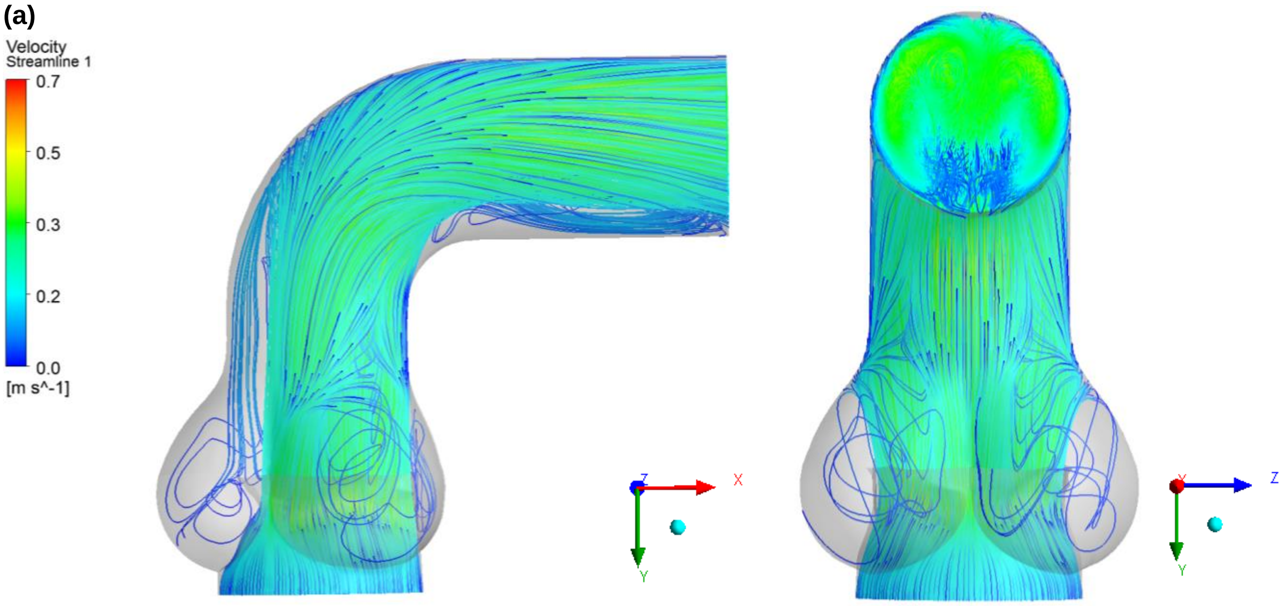

(b)

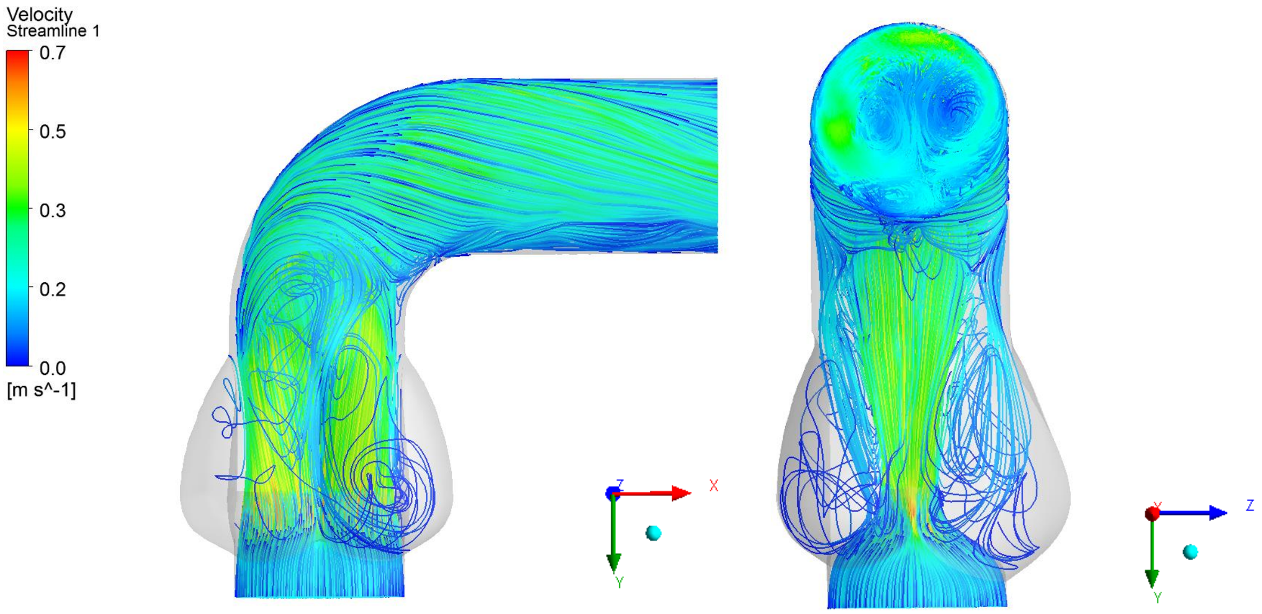

(c)

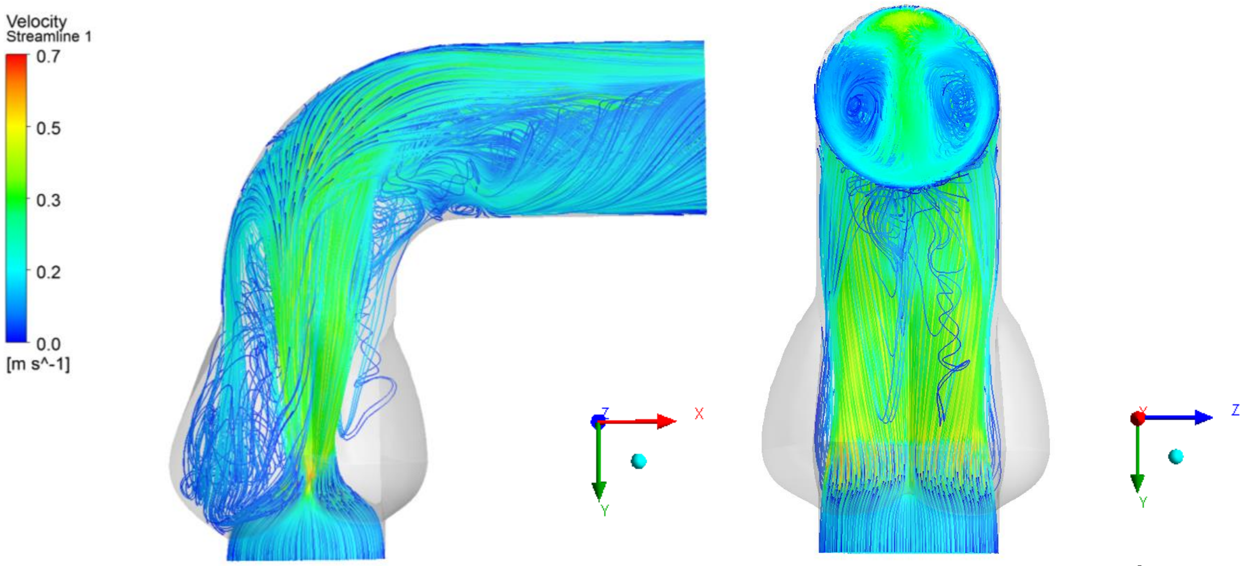

Figure 9. Pathlines colored by velocity magnitude of (a) model of tricuspid valve, (b) model of BAV left-right fusion and (c) model of BAV left-non fusion.

As expected, once the blood flow strikes against the outer wall of the aorta in the aortic arch, the profile drastically changes trying to follow the shape of the walls and it creates the so called Dean vortices (visible at the outlet of the three models).

3.2 Velocity Vectors

Velocity vectors plots of the models are shown in figure 10 (a) – (c). The range displayed has been modified to be the same on every plot and simplify the comparison.

(a)

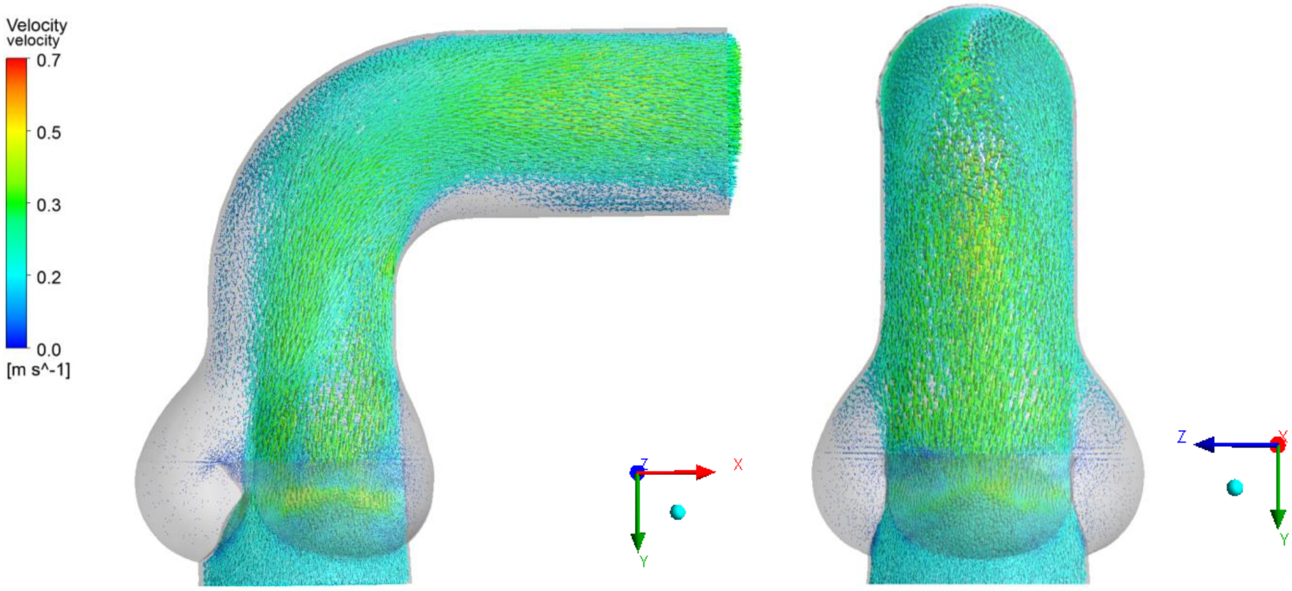

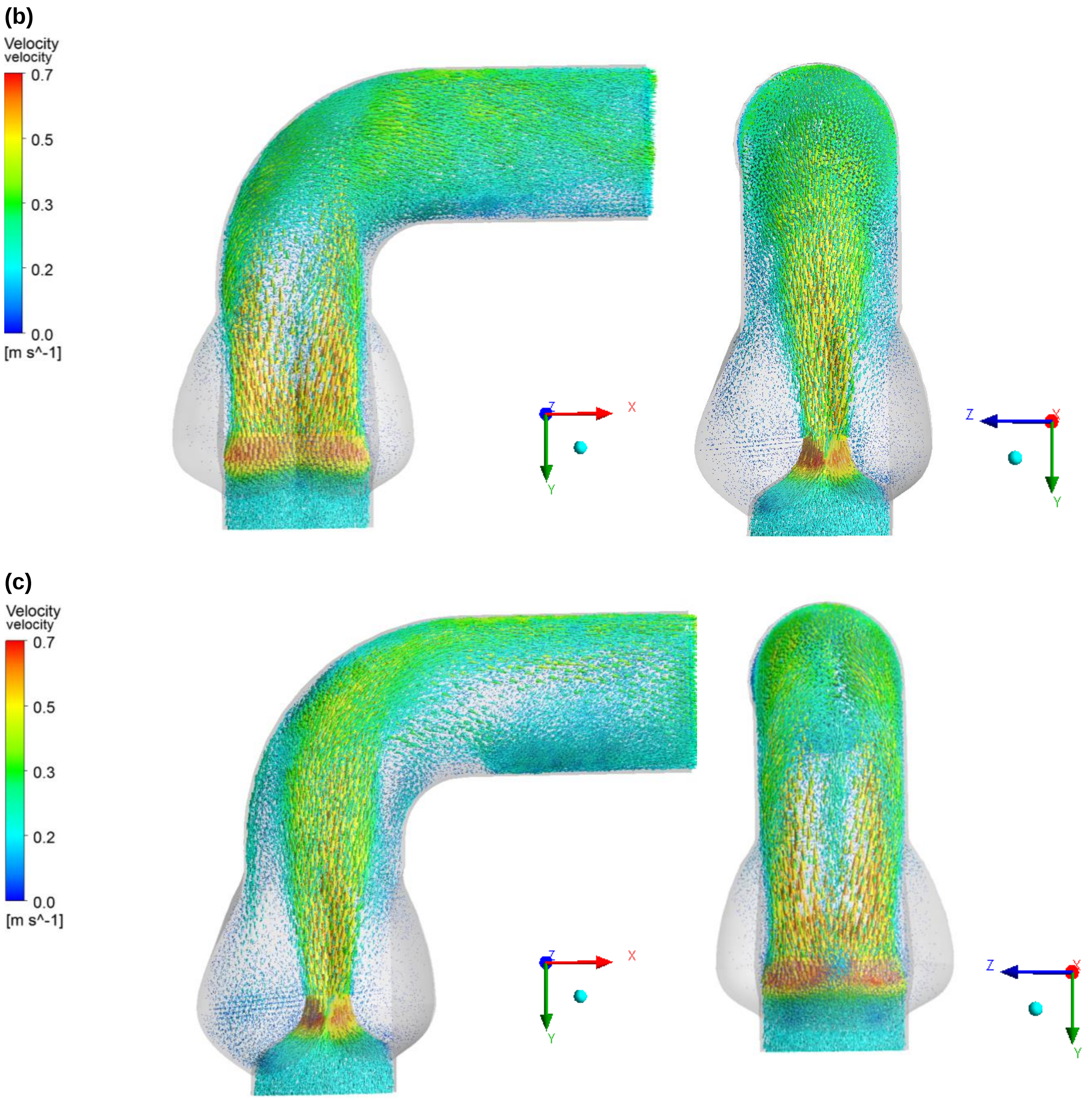

Figure 10. Velocity vectors plot colored by velocity magnitude of (a) model of tricuspid valve, (b) model of BAV left-right fusion and (c) model of BAV left-non fusion.

As expected from the results of the streamlines, the distribution of the velocity gradient varies highly from one model to another. Please notice that the recirculating vortices formed in the sinuses of Valsalva have in all cases a relatively low velocity.

The separation of the boundary layer after the aortic arch is clear on the tricuspid case, whereas it appears that the boundary layer doesn't fully form on the bicuspid valve cases.

3.3 Pressure Contours

Pressure contours of the three models are shown in figure 11 (a) – (c). The range displayed has been modified to be the same on every plot and simplify the comparison.

It is important to notice that the range of values for the pressure in consistent with the mean arterial pressure for the aorta which is known to be approximately 13332.2 Pa. Again, it is also important to keep in mind that we are taking into account a mean average flow rate of approximately 5 Lpm, and that these results will vary throughout the cardiac cycle.

(a)

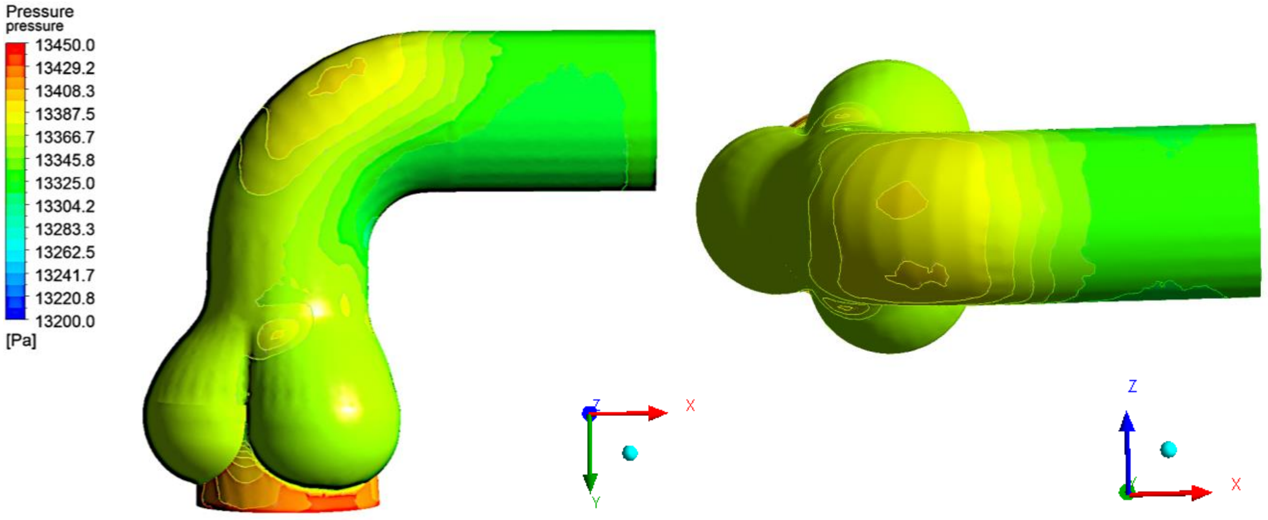

(b)

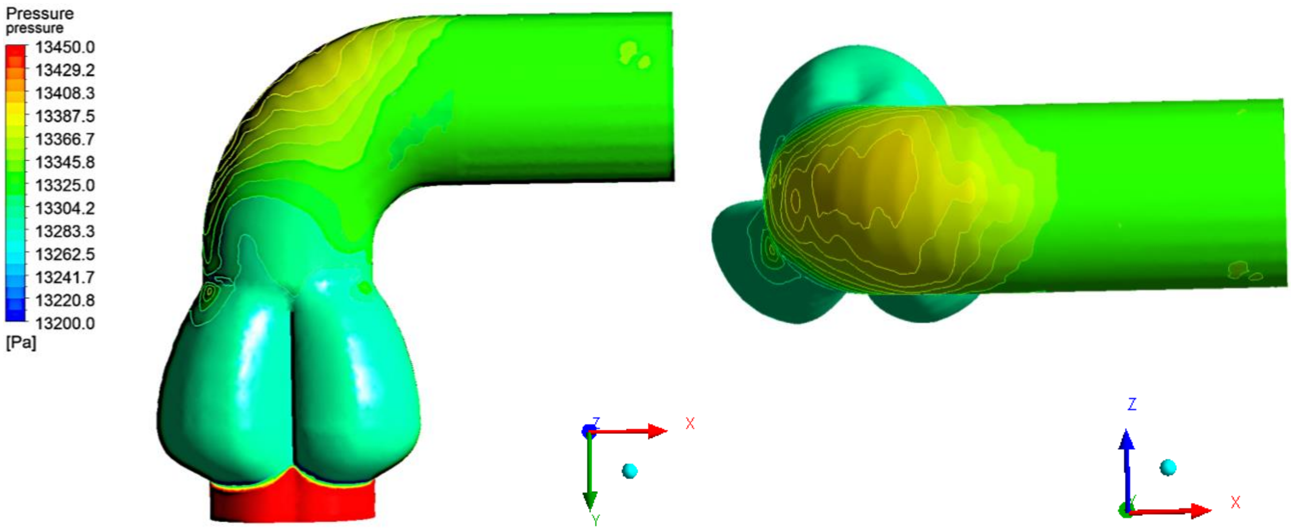

(c)

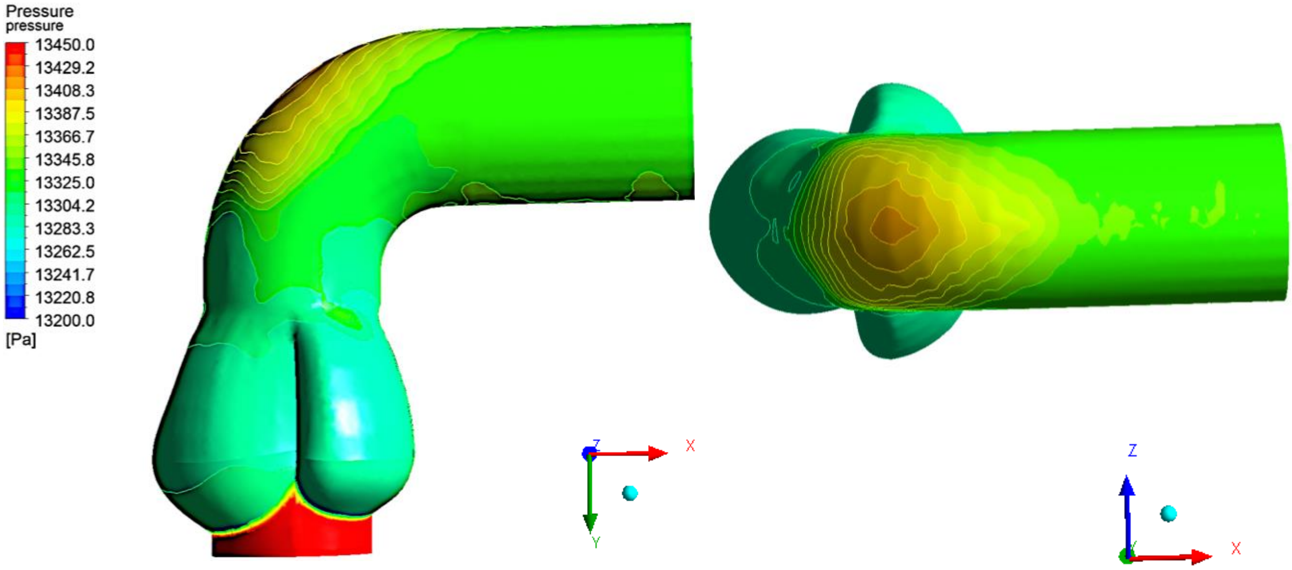

Figure 11. Pressure contours of (a) model of tricuspid valve, (b) model of BAV left-right fusion and (c) model of BAV left-non fusion.

3.4 Wall Shear Stress

Wall shear stress contours of the three models are shown in figure 12 (a) – (c). The range displayed has been modified to be the same on every plot and simplify the comparison.

As expected from the results obtained for velocity gradients, there is a wall shear stress gradient in all three cases, with a considerably higher shear stress on the outer wall than the inner wall of the aortic arch. Likewise, the focalized areas with peak wall shear stress correlate with the areas where peak velocities were registered.

(a)

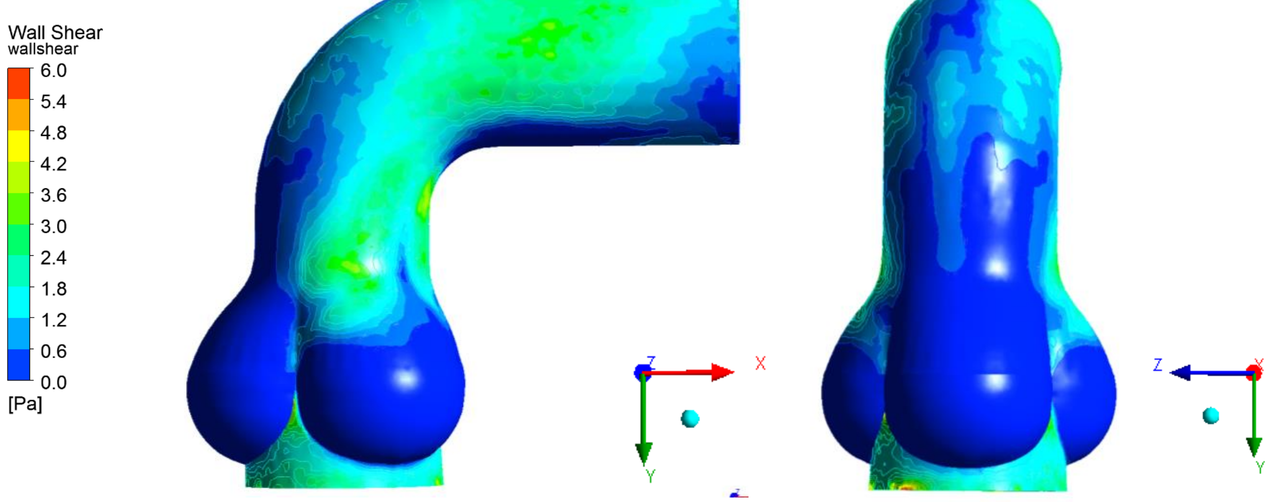

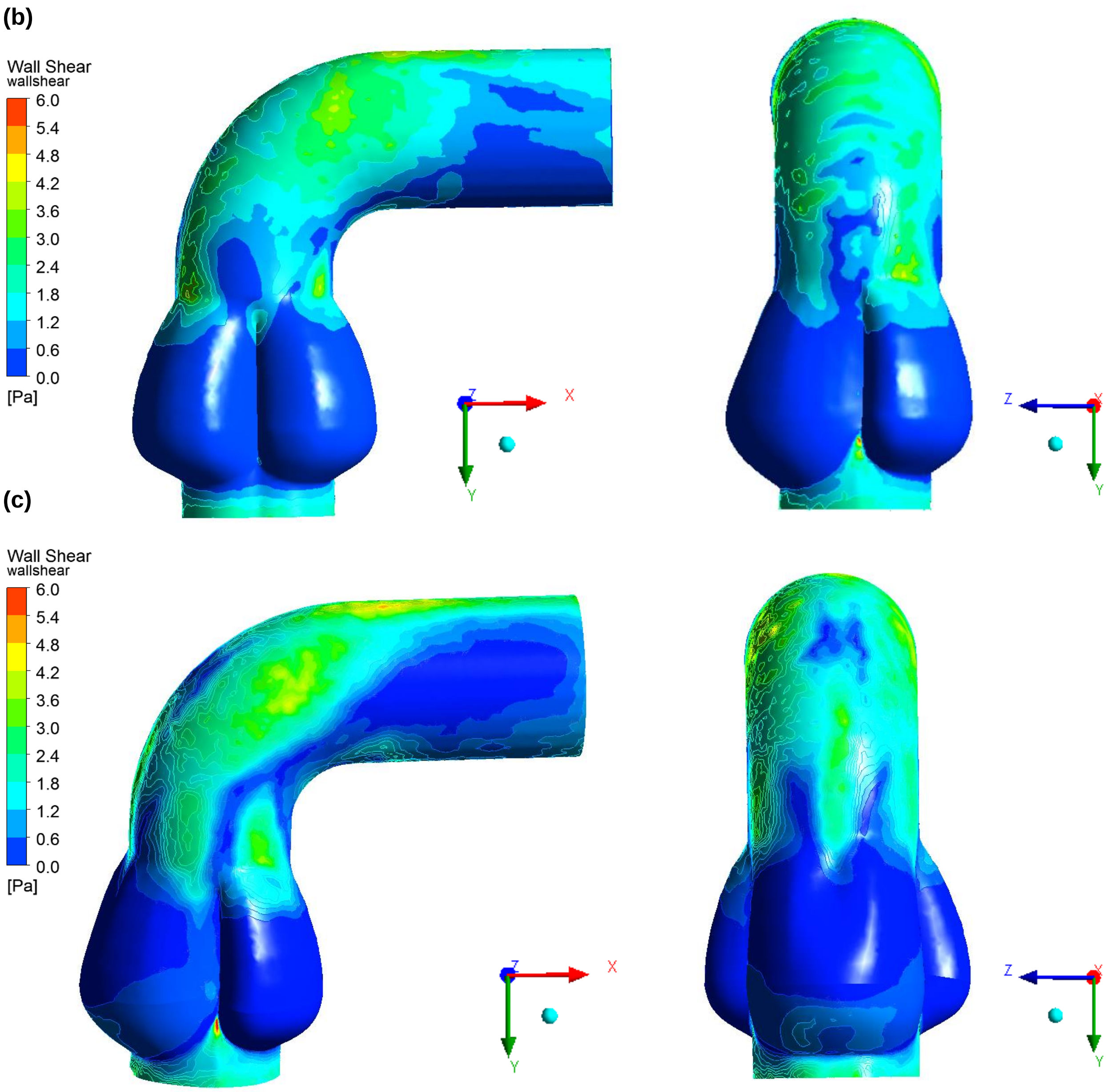

Figure 12. Wall shear stress contours of (a) model of tricuspid valve, (b) model of BAV left-right fusion and (c) model of BAV left-non fusion.

3.5 Pressure drop vs. flow rate

Figure 13 shows a graph representation of the pressure drop (in Pa) between inlet and outlet versus the blood flow rate (in L/min) in the aorta for the three models. In order to create this graph, two extra analyses have been performed in each geometry by keeping the previous conditions and solely altering the inlet velocity.

These curves feature the pressure drop of each geometry when Q ≈ 0, 3, 5 and 20 L/min. Due to complications with the software, in order to expand the curve to the greatest possible flow rate (20 L/min), MATLAB software has been used to obtain the corresponding equations and the pressure drops for Q = 20 L/min have been extrapolated from the data.

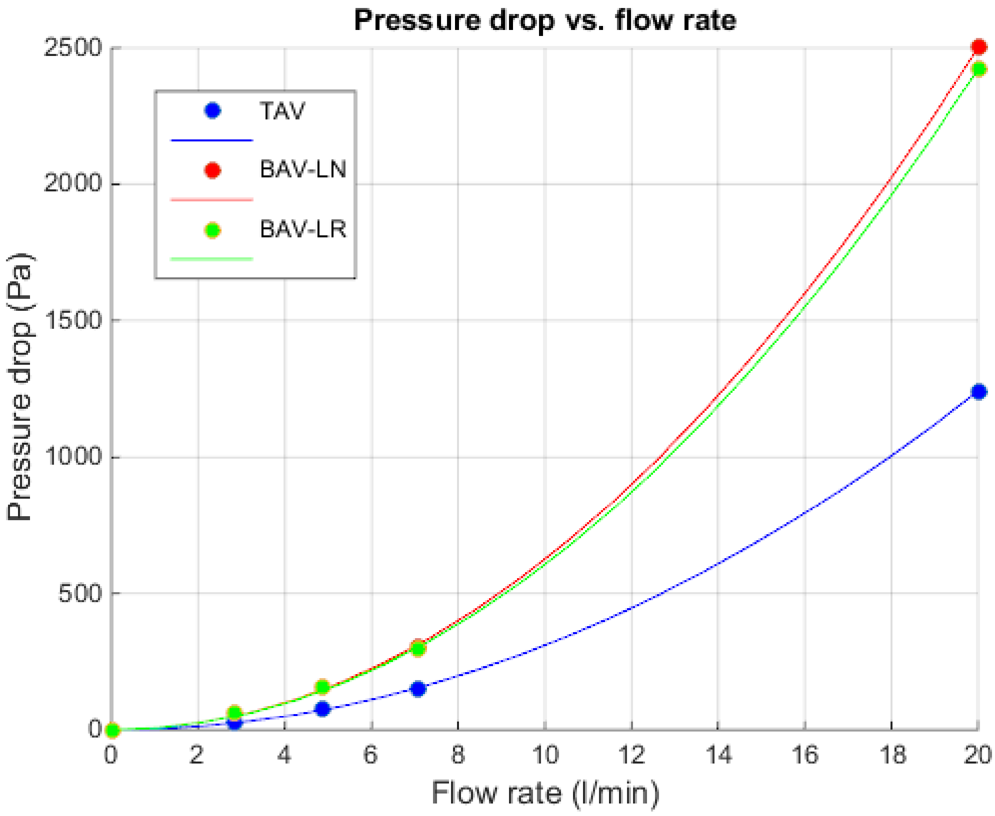

Figure 13. Graph representation of Pressure Drop (Pa) vs. Flow Rate (L/min) for the three models.

DISCUSSION

The results obtained from the analyses follow what was expected from previous MRI-based studies and the general behavior of a fluid on a curve pipe.

Figures 9 (a) – (c) show streamlines generated for each one of the three cases. Even though all the geometries show great levels of recirculating flow in the sinus of Valsalva, the profiles of the flow show differences. These variations can be partially justified by the changes in the geometries of the sinuses, but are mainly due to the changes in the geometries of the leaflets. The variation of the ejection profile causes the recirculating flow to vary. Studies have shown that variations of these recirculating flows can cause partial instability of the flow, which could lead to clinical consequences[14].

The reduction in the area of the inlet prevents the fluid from filling the aorta while ascending towards the arch, which leads to large areas of abnormal recirculation. This phenomenon alters the regular haemodynamics changing the distribution of the pressure and wall shear stress along the aorta, which could potentially lead to clinical consequences.

These pathlines show that tricuspid valves allow for the maximum dispersion of the blood flow in the aorta and lower velocity magnitude, which will result in higher areas of distribution of the pressure and wall shear stress.

It is important to notice that the models for the two different types of bicuspid valves yield considerably different pathlines, which could potentially explain the differences in frequency, magnitude and character of the vascular complications associated with the different forms of bicuspid aortic valves.[12]

Figures 10 (a) – (c) show velocity vector plots generated for each one of the three cases. It is clear that, even though the distribution is turned 90 degrees, the magnitude of the peak velocities for the both cases of bicuspid valve are very similar. In both models, the peak velocity reaches approximately 0.7 m/s and it is focused on the center of the aorta directly after the valves. This is an approximately 400% increase in the velocity set on the inlet (0.17 m/s).

Tricuspid valve model shows a peak velocity of 0.4 m/s approximately, almost half of the velocity obtained from BAV models. These great differences can be explained by the conservation of mass principle (equation 6), which stipulates that on the study of steady flow through rigid pipes, the volumetric flow rate must be constant. The difference in effective orifice area between the stenotic valves and the normal valves produces an increment in the velocity in order to follow this principle.

$$Q = A\vec{u} = \text{constant} \qquad \textbf{[equation 6]}$$

As explained previously, the curve obliges the flow to change direction, forcing the axial velocity profile to become skewed toward the outer wall, and as the curvature continues, the high velocity regions impact the outer wall and the profile acquire a circumferential component forming the Dean vortices. This phenomenon explains the presence of a much higher velocity magnitude on the outer wall than the inner wall, for all the cases. Girdauskas et al[12] determined that the perturbations in the blood flow due to BAV were the character eccentric and directed toward the outer wall, which agrees with the results of this study.

Figures 11 (a) – (c) show pressure contours generated for each one of the three cases. Distribution varies greatly between the models, but pressure remains approximately on the same range. As expected, the tricuspid valve model shows a distributed pressure along the aortic arch, with the peak pressure situated at the end of the curved area, where the Dean vortices are formed. Both bicuspid valve models, however, show a more focalized pressure peak at the center of the wall due to smaller area of the orifice of ejection.

Figure 12 (a) – (c) show wall shear stress contours generated for each one of the three cases. The figures show a visible gradient of wall shear stress in the lumen of the aorta, with higher values on the outer wall, and lower on the inner. This gradient is due to the curvature of the aorta that obliges the flow to change directions one it hits the outer wall. As explained before, this causes a higher velocity in the outer wall, which leads to higher wall shear stress.

Barker et al[16] assessed wall shear stress along the lumen of the ascending aorta with MRI and determined that the distribution and magnitude of wall shear during systole is significantly different between patients with TAV and patients with BAV. Patients with BAV shown higher levels of wall shear than TAV patients. These results support the results obtained from the present study.

The graph shown in figure 13 represents the curves pressure drop vs. flow rate generated for each model. It is evident that all three curves follow a parabolic distribution, that is, all curves follow an equation of the form shown in equation 7. This type of relation was expected on these geometries.

$$\Delta P = kQ^2 \qquad \textbf{[equation 7]}$$

An increment in pressure drop is due to an increment in the resistance to the flow, which leads to higher wall shear stress and other complications. In other words, the lower the resistance the lower the pressure drop and therefore the better the flow properties of the model. The abovementioned graph shows a clearly advantage of the TAV model over the two BAV cases, as was expected. It also shows a slight difference between the two types of BAV, being the BAV left-non fusion the one with the higher pressure drop-flow rate curve and consequently the worse haemodynamics.

4.1 Conclusion

This study has analyzed three different geometries of the aortic root and aortic arch (one physiologically normal, one bicuspid valve due to a left-right leaflets fusion, and one due to a left-non leaflets fusion) in order to determine the possible relation between the variation in the haemodynamics of the blood flow due to bicuspid aortic valve condition, and the development of aortic dissection type A.

The analyses performed show that BAV alters significantly the physiological haemodynamics of the aorta causing an increment in the resistance to the flow. It is important also to acknowledge that it has been proven that different types of BAV yield different results and could potentially cause different pathologies or different forms of the same pathology.

The combination of high pressure and high wall shear stress in areas where these conditions are not present on patients with TAV may lead to a deformation or abnormal distention of the outer wall, which could lead to weakening of the intima, facilitating the formation of the tear in the wall that is known to be the first phase of aortic dissection[2]. This conclusion agrees with the study carried out by Green et al 2003, which appoints hypertension of the aorta as the main mechanical cause of aortic dissection.

4.2 Limitations of the study

Some of the assumptions made for this study do not fully correspond with the physiological situation, even though all of them seem to be reasonable. As previously explained, the rheology of the blood follows a Casson's relation, and not a Newtonian relation; the aorta, as any other blood vessel, has some level of distensibility that was neglected when rigid walls were assumed.

In addition, the geometries did not take into consideration the effect of the coronaries arteries, nor the cephalic arteries, and did not represent the physiological curvature of the aortic arch. Finally, not all types of BAV were considered for this study but we have shown that different types, lead to different haemodynamics.

Study of the models using pulsatile flow was attempted but failed. These analyses where intended to be performed with a simple sine wave slightly modified to fit the desired velocity profile. However, this does not yield realistic results since the actual pulsatile wave of the heart has a very characteristic shape. This shape causes that, even though the flow reaches high Reynolds number that would theoretically lead to turbulences, these peaks are so instantaneous that the turbulences do not have time to form before the Reynolds numbers goes down to laminar levels. In order to obtain the abovementioned wave form, Fourier series should be used, however, due to the nature of the study and lack of time, these analyses were finally dismissed as not essential.

4.3 Future work

In order to obtain more accurate results, pulsatile flow could be study to assess the consequences of BAV through out the entire cardiac cycle. Also wall distensibility could be taken into consideration, although that would imply using dynamic meshes, which will suppose a significant increment of the computational cost. In addition to this, a finer mesh should be use, however that leads to the necessity of using a non-scholar version of Ansys Fluent and running the models in parallel in a cluster of computers in order to minimize the increment in computational cost.

Finally, clinical data should be analyzed and compared with the results from the idealized geometry in order to validate them and provide a more in depth knowledge of the phenomenon.

REFERENCES

1. Chandran, Krishnan B., Stanley E. Rittgers, and Ajit P. Yoganathan. *Biofluid mechanics: the human circulation.* CRC Press, 2012.

2. Green G Ri , Kron I Li . (2003) *Chapter 45: Aortic Dissection*. In: Cohn LH, Edmunds LH Jr, eds. Cardiac Surgery in the Adult. New York: McGraw-Hill.

3. Stevens, L.M., Madsen, J. C., Isselbacher, E. M. et al. (2009) *Surgical management and long-term outcomes for acute ascending aortic dissection*. The Journal of Thoracic and Cardiovascular Surgery. **138** (6), 1349 – 1357.

4. Wiesenfarth, J. M. (2011, May 24) Emergent Management of Acute Aortic Dissection. Medscape. Retrieved 10/22/2012 from http://emedicine.medscape.com

5. Betts, J. Gordon (2013). *Anatomy & physiology*. pp.787 – 846.

6. Unknown. *The Cardiovascular System.* Retrieved 01/18/2015 from http://www.starsandseas.com

7. Cleveland Clinic. *Aortic dissection*. Retrieved 01/27/2015 from http://my.clevelandclinic.org/

8. MedMovie. *Aorta*. Retrieved 02/06/2015 from http://medmovie.com

9. University of Florida Health. Aortic dissection. Retrieved 02/06/2015 from https://ufhealth.org/

10. Charitos EI, Sievers HH. *Anatomy of the aortic root: implications for valve sparing surgery*. Ann Cardiothorac Surg 2013; **2**(1):53-56.

11. Valley Health System. *Bicuspid Aortic Valve.* Retrieve 03/10/2015 from http://valleyheartandvascular.com

12. Girdauskas, E. et al (2014). *Bicuspid Aortic Valve and Associated Aortopathy: An Update*. Semin Thoracic Surg. **25**. Pp. 310 – 316.

13. Sadron Blaye-Felice, M. et al. (2012) Usefulness of three-dimensional transthoracic echocardiography for the classification of congenital bicuspid aortic valve in children. European Heart Journal. **13**. pp. 1047 – 1052.

14. Peacock, J. A. (1990). *An In Vitro Study of the Onset of Turbulence in the Sinus of Valsalva.* Circ Res. **67**. pp. 448 – 460.

15. Cotrufo M, Della Corte A. (2009) *The association of bicuspid aortic valve disease with asymmetric dilatation of the tubular ascending aorta: Identification of a definite syndrome.* J Cardiovasc Med. 10. pp. 291-297.

16. Barker AJ, Lanning C, Shandas R (2010). *Quantifica- tion of hemodynamic wall shear stress in patients with bicuspid aortic valve using phase- contrast MRI*. Ann Biomed Eng. 38. pp. 788-800.

17. Sievers, H. & Schmidtke, C. (2007). *A classification system for the bicuspid aortic valve from 304 surgical specimens.* The Journal of Thoracic and Cardiovascular Surgery. **133**. pp. 1226 – 1233.